Computational models of the single substitutional nitrogen atom in diamond

2003 J. Phys.: Condens. Matter 15 3135

(http://iopscience.iop.org/0953-8984/15/19/314)

INSTITUTE OF PHYSICS PUBLISHING JOURNAL OF PHYSICS: CONDENSED MATTER

J. Phys.: Condens. Matter **15** (2003) 3135–3149 PII: S0953-8984(03)58741-0

Computational models of the single substitutional nitrogen atom in diamond

E B Lombardi[1], Alison Mainwood[2,4], K Osuch[3] and E C Reynhardt[1]

[1] Faculty of Science, University of South Africa, 0003, PO Box 392, South Africa
[2] Physics Department, King's College London, Strand, London WC2R 2LS, UK
[3] Physics Department, University of South Africa, 0003, PO Box 392, South Africa

E-mail: alison.mainwood@kcl.ac.uk

Received 23 January 2003, in final form 31 March 2003
Published 6 May 2003
Online at stacks.iop.org/JPhysCM/15/3135

Abstract

The single substitutional nitrogen atom in diamond is apparently a very simple defect in a very simple elemental solid. It has been modelled by a range of computational models, few of which either agree with each other, or with the experimental data on the defect. If the computational models of less well understood defects in this and more complex materials are to be reliable, we should understand why the discrepancies arise and how they can be avoided in future modelling. This paper presents an all-electron, augmented plane-wave (APW) density functional theory (DFT) calculation using the modern APW with local orbitals full potential periodic approximation. This is compared to DFT, finite cluster pseudopotential calculations and a semi-empirical Hartree–Fock model. Comparisons between the results of these and previous models allow us to discuss the reliability of computational methods of this and similar defects.

1. Introduction

In the last few decades, the experimental data on defects in semiconductors have become so sophisticated that it is sometimes possible to derive a full structural and electronic model of a defect from experimental data alone. However, more often the experiments can be interpreted ambiguously or the data are not conclusive, and additional sources of information are needed. Here, quantum mechanical modelling of defect centres plays an important role. All computational modelling of quantum mechanical systems necessarily involves approximation at some level [1, 2]. It is useful to know which computational models can reliably predict which properties of the defects. This paper takes one of the simplest elemental solids, diamond, and one of the simplest possible defects in it, and shows how the large number of computational models, including *ab initio* calculations, do not agree with each other or with the experimental

[4] Author to whom any correspondence should be addressed.

data on this well characterized defect. If we are to trust calculations on much less well understood, much more complex defects in this and other materials, it would be sensible to understand why these discrepancies occur and whether they can be avoided.

Nitrogen is the most common impurity in diamond. It is incorporated in single substitutional form in the lattice (most synthetic and some rare natural diamonds, which are classified as type Ib [3]). Under high temperature and pressure, in natural geological conditions or in the laboratory, various aggregates may form (A and B centres, in diamonds classified as type Ia) [4], or the nitrogen may combine with other defects [5].

The single substitutional nitrogen atom, sometimes known as the C centre, has a distinctive infrared spectrum with a local vibrational mode at 1344 cm^{-1} [6] and gives rise to the P1 electron paramagnetic resonance (EPR) signal. The P1 centre was first identified in 1959 with a single substitutional nitrogen atom [7]. It gives rise to a deep level in the bandgap of diamond [8] and not the shallow donor level that might be expected, based on comparison with P in silicon.

Since the 1960s very many experimental and theoretical studies have been carried out on this defect. While experimental studies have generally been in agreement with each other, the same cannot be said of the significant number of theoretical calculations that have been performed for this centre. Experimentally it has been well established that one of the four N–C bonds elongates, producing a C_{3v} symmetry for the centre. However, several theoretical treatments (both *ab initio* and semi-empirical) have predicted that the nitrogen stays on site, giving a T_d symmetry. Even among those theoretical models that predict the experimentally observed symmetry, there is little agreement on the energy, or even number, of electronic levels in the bandgap.

Various explanations have been put forward to rationalize the C_{3v} distortion of the defect. Originally, it had been ascribed to the occupation of an antibonding orbital by the fifth valence electron of the N atom [7], while a spontaneous Jahn–Teller distortion has also been put forward [9]. The origin of the relaxation has also been visualized [10, 11] as a lone pair orbital on nitrogen and a dangling bond orbital on a carbon atom directed towards each other, the gap state corresponding to an antibonding combination of these two orbitals.

In this paper, we compare some of the very many computational models of the single substitutional nitrogen atom in diamond and report new calculations using semi-empirical methods with large clusters [2, 12] and state-of-the art all-electron, linearized augmented plane-wave (APW) density functional theory (DFT) as well as the APW + lo full potential periodic formalism using WIEN2k [13], together with DFT calculations on finite clusters using the AIMPRO program [14].

1.1. Experimental properties

Nitrogen is one of the most common impurities in diamond, with concentrations varying from 0.01 ppm in type II diamonds (those with very low nitrogen content) to 5000 ppm (atomic) in type Ia stones [3].

The results of early measurements of EPR and ENDOR spectra of the P1 centre have previously been reviewed [15]. More recent EPR and ENDOR studies include [16] and [17], while the quadrupole interaction in this centre has also been studied [18]. Importantly, these studies show that the P1 centre has C_{3v} symmetry with the nitrogen atom relaxing away in a $\langle 111 \rangle$ direction from one of its neighbours and with most of the unpaired spin located at the unique carbon neighbour, while the spin density at the nucleus of the N atom is greater than the spin density at the nucleus of the unique carbon atom. The EPR spectrum of the P1 centre has an isotropic Zeeman splitting g-tensor of 2.0024, which is close to the free electron value.

Measurements of the electrical resistance of type Ib diamonds as a function of temperature [8] indicate that the impurity energy level of nitrogen is 1.7 eV below the conduction band of diamond, while from optical absorption and photoconductivity experiments the optical ionization energy is closer to 2.2 eV [8, 19]. The difference in these values indicates that the relaxation of the structure in the ground state is very large, accounting for up to 0.5 eV difference in energies.

Of the other studies that have been carried out on the P1 centre in diamond, information on the barrier heights comes from orientation of the centre under uniaxial pressure and relaxation at high temperature [20] as well as motional averaging studies at high temperatures [21]. Temperature dependences of spin–spin and spin–lattice relaxation times have also been studied [22, 23], where it has been shown that cross relaxation between different impurity centres is important, this mechanism being more effective than the direct mechanism in some cases. Studies of type Ib diamond with high nitrogen concentrations ($[N_s] > 300$ ppm) [24] show that for closely separated pairs of P1 centres the constituent centres have certain determined relative orientations. It is inferred from these data that the interaction between pairs of P1 centres closer than 0.4 nm is strong enough for them to be coupled to give a net zero spin with the exception of the configuration of two P1 centres situated directly above one another in a [001] direction, separated by four atomic layers. Random relative orientation occurs for separations of 0.7 nm or more. The interaction between P1 centres has been explained by treating nitrogen centres as point magnetic dipoles, with the long distance interaction occurring via the magnetic dipole–dipole interaction.

1.2. Previous theoretical treatments

Sixteen computational models of single nitrogen in diamond are summarized in table 1, which includes four from the present work. It is clear that, at the very least, a plausible model of the centre should reproduce the C_{3v} symmetry, the deep donor level near 2.2 eV below the conduction band (from the optical ionization energy of 2.2 eV [19], since the thermal ionization energy of 1.7 eV [8] implicitly includes any subsequent relaxation of the ionized donor), together with the spin distribution localized on the unique carbon atom. If it also casts light on the *origin* of the C_{3v} distortion, this would be an added benefit. We focus mainly on the more modern DFT calculations and include various older models for the sake of completeness.

1.2.1. Semi-empirical calculations. The first extensive calculations on the single nitrogen substitutional atom in diamond were performed by Messmer and Watkins [9] using a noniterative (non-self-consistent) extended Hückel theory (EHT) method. They found a triply degenerate, singly occupied, deep impurity energy level of T_2 symmetry, 2.2 eV above the valence band edge. The C_{3v} distortion of the centre was ascribed to a spontaneous Jahn–Teller distortion. Further calculations [25], using a self-consistent HF–LCAO–MO-type calculation, found a similar level in the gap, but this time 2.1 eV below the conduction band. It was shown [26] that, depending on the parametrization of the EHT method, the A_1 and T_2 levels can be reversed, leading to a single electron occupying a nondegenerate A_1 level in the bandgap. Similar calculations were performed [27–29] using a CNDO semi-empirical technique in a nonperiodic cluster, with the results dependent on cluster size, but all showing a substantial C_{3v} distortion.

1.2.2. Hartree–Fock calculations. Unrestricted Hartree–Fock cluster calculations [30] found an elongation of 0.3 Å ($\sim$20%) for the C–N bond. The antibonding, triply degenerate T_2 state

Table 1. Calculations reported for the single nitrogen substitutional atom in diamond. The one-electron energy levels are relative to the edge of the conduction band (E_C) or valence band (E_V), together with their degeneracy and occupancy. For spin polarized calculations, the spin splitting of the one-electron levels is given in brackets.

			A lattice site			C_{3v} symmetry		
References	Method	Elongation of N–C bond	One-electron levels	Degen.	Occ.	One-electron levels	Degen.	Occ.
[9]	EHT	26%	$E_C - 1.5$ eV	$T_2(3)$	1	$E_V + 2.2$ eV +2 close to bands		
[25]	HF–LCAO–MO (finite cluster)	∼5%	$E_C - 1.26$ eV	$T_2(3)$	1	$E_C - 2.1$ eV		
[27]	CNDO (finite cluster)	5–10%						
[29]	CNDO (finite cluster)	24–25%						
[32]	DFT—Green function LDA (periodic)		$E_C - 0.15$ eV	$A_1(1)$	1			
[30]	UHF–SCF (finite cluster) spin-polarized	19%		$T_2(3)$ $A_1(1)$	1			
[31]	DFT, LDA (finite cluster)	0%	$E_C - 0.9$ eV +T_2 state in CB	$A_1(1)$	1			
[33]	LDA (periodic)	Fixed at lattice site	$E_C - 0.8$ eV	$A_1(1)$	1			
[10]	DFT, plane waves (periodic)	25%	$E_C - 0.7$ eV	$A_1(1)$	1	$E_C - 1.9$ eV $E_V + 0.15$ eV		1 2
[11]	DFT, LDA (finite cluster)	28%	Midgap	$A_1(1)$	1	$E_C - 0.5$ eV $E_V + 1.2$ eV		1 2
[34]	Molecular dynamics (periodic)	N at lattice site; C relax 35%	$E_C - 0.17$ eV		1	$E_C - 3.4$ eV		1
[10]	MNDO	0%						
This work	UHF AM1 (96-atom supercell), spin polarized	0%	$E_V + 1.7$ eV	$A_1(1)$	1			
This work	DFT–LSDA (finite, 165 atoms), spin polarized	32.9%	$E_C - 0.46$ eV (0.07 eV)	1	1	$E_C - 0.71$ eV (0.58 eV) $E_V + 0.26$ eV (0.16 eV)	1 1	1 2
This work	FLAPW GGA (8-atom supercell), spin polarized	21.2%	$E_C - 1.0$ eV $E_C - 2.75$ eV	1 1	1 2	$E_C - 0.66$ eV $E_V + 0.85$ eV (∼0.01 eV)	1 1	1 2
This work	APW + lo GGA (64-atom supercell), spin polarized	28.1%				$E_C - 1.89$ eV (0.82 eV)	1	1

(unoccupied) was above the nondegenerate, singly occupied A_1 state, so here the Jahn–Teller effect could not have been responsible for the lowering of symmetry.

1.2.3. Density functional theory calculations on finite clusters. In local density approximation (LDA) DFT calculations [31], two impurity related states were observed: an A_1 state of s-like character (antibonding nature), at $E_C - 0.90$ eV, and a T_2 state of p-like character, just above the bottom of the conduction band. The undistorted configuration was stable. In other pseudopotential LDA DFT calculations (using the program AIMPRO) [11], the N–C bond length was found to elongate by 28%.

1.2.4. Density functional theory calculations with periodic clusters. DFT calculations [32], using a Green function self-consistent local density functional method, found a singly occupied, nondegenerate A_1 level 0.15 eV below the minimum of the conduction band, together with an unoccupied, triply degenerate T_2 level in the conduction band. Since no partially occupied, degenerate levels were induced, this confirmed that the distortion of the single substitutional nitrogen atom in diamond was not due to a Jahn–Teller effect.

LDA DFT calculations [33], with the substitutional nitrogen atom fixed at the lattice site, found a state 0.8 eV below the conduction band minimum. Other calculations with plane wave methods and *ab initio* pseudopotentials [10] found that the N–C bond length increased by 25%. Results were dependent on cluster size, though not on the number of k-points (for a cluster of 64 atoms). An occupied orbital was found at $E_V + 0.15$ eV. The EPR-active orbital was located at $E_C - 1.9$ eV, consisting of an antibonding combination of the nitrogen lone pair and carbon dangling bond orbitals. The nitrogen atom was, however, also found to remain at the lattice site in other more recent *ab initio* calculations [34]. The four carbon nearest neighbours were found to relax strongly away from the nitrogen, the N–C bond lengths each increasing by 35%, retaining T_d symmetry for the centre. The spin density, however, did have C_{3v} symmetry, which would be in agreement with EPR experiments.

Studies of the single substitutional nitrogen atom near a surface have also been carried out [35], where it has been found that the extra electron plays a crucial role in the bond-breaking of the unique N–C bond.

1.2.5. Discussion of the previous models. A model for the origin of the distortion emerges from [10] and [11], the two models which, so far, reproduce the experimental data best. Consider the valence electrons of the nitrogen atom and the unique carbon atom: both the nitrogen and unique carbon atoms bond with three of their carbon neighbours. On the N atom the remaining two valence electrons occupy a lone-pair orbital, while on the unique carbon atom the fourth valence electron occupies a dangling bond orbital. The nitrogen's lone-pair orbital and the carbon's dangling bond orbital are directed towards each other, forming bonding and antibonding orbitals from the sp^3 hybrids. The lower bonding orbital will be fully occupied, with N and the unique C atoms each contributing an electron, while the partially occupied gap state corresponds to an antibonding combination of these two orbitals.

It is seen from table 1 that even DFT calculations yield cases where no deviation from T_d symmetry was observed (as was the case with older semi-empirical calculations). The impurity energy levels are predicted to be almost anywhere in the energy gap, and though DFT methods have a higher likelihood of finding two impurity energy levels in the gap, there is no general agreement. Finally, many authors report that their results were dependent on cluster size.

2. The present models of the defect

We have performed calculations using accurate semi-empirical Hartree–Fock methods with large clusters (MOPAC 93), DFT pseudopotential methods with finite clusters using the AIMPRO program and *ab initio* all-electron, linearized APW GGA–DFT, as well as the APW + lo full potential periodic formalism using WIEN2k.

2.1. Semi-empirical Hartree–Fock calculations

Because semi-empirical methods use fewer computer resources, much larger clusters of atoms can be used. They could, therefore, indicate whether size effects are causing the anomalous results referred to in section 1.

In these calculations, the advanced LCAO AM1 Hamiltonian (based on the MNDO formalism), implemented in MOPAC 93 [2, 12], was used. We used a periodic supercell of 96 carbon atoms consisting of eight layers each of 12 atoms for the full calculations, with Born–von Karman periodic boundary conditions. A similar periodic supercell of 192 atoms was also used, but with fewer atoms allowed to relax in the geometry optimization. Note that the 192-atom calculation is the first to be performed where the nitrogen concentration is comparable with the highest seen experimentally. The results for the larger cluster are given in brackets, below. The lattice constant was optimized, keeping the symmetry of the cluster fixed, giving a value of 3.5623 Å, close to the experimental value of 3.5667 Å [36]. The bandgap at the Γ-point was calculated to be 10.0 eV (9.8 eV), compared to the experimental value of 7.3 eV (the direct bandgap).

Using these clusters, replacing a carbon atom with nitrogen and keeping the lattice constant at the experimental value, the geometry was optimized for various initial atomic positions, allowing the impurity atom, its neighbours and next nearest neighbours to relax. In all calculations, the nitrogen substitutional atom was stable at the lattice site. Even when the nitrogen and a neighbouring carbon atom were displaced along $\langle 111 \rangle$ directions, the atoms relaxed back to T_d symmetry. There was a nondegenerate impurity level in the bandgap at 1.7 eV (2.1 eV) above the top of the valence band (highest occupied pure carbon orbital). This impurity level in the bandgap consists of the valence s orbital of the nitrogen atom overlapping with the sp^3 hybrid orbitals of the four carbon neighbours. The spin density, therefore, has T_d symmetry. The carbon atoms are bonded with the usual sp^3 orbitals, while the nitrogen atom bonds only with its p orbitals, and the s orbital contains the unpaired spin.

The results varied very little with cluster size. Comparing the nitrogen–nitrogen distances in these periodic clusters, 7.1 Å (10 Å), with those seen experimentally where the impurities are known to interact (<7 Å), we are confident that the interaction between nitrogen atoms in the periodic clusters is unlikely to be responsible for the poor results.

2.2. Ab initio density functional theory, with finite clusters

The single substitutional nitrogen atom in diamond was also modelled using local density functional theory (LDA) with norm-conserving Bachelet–Hamann–Schlüter pseudopotentials [37], as implemented in the AIMPRO code [14]. Finite, hydrogen terminated clusters of 165 C atoms were used, bounded by (111) surfaces. This was the same computational method as that used by [11], except that their clusters contained only 45 C atoms. The N atom was placed at the centre of the cluster. All atoms up to third neighbours from the nitrogen atom were allowed to relax and the clusters were not restricted to any predetermined symmetry.

Firstly, the nitrogen atom was placed on a lattice site and a full geometry optimization performed without any symmetry constraints. The final geometry was found to have T_d symmetry, with the N atom remaining on the lattice site and the carbon neighbours relaxing away from it by 0.1 Å, increasing the N–C bond lengths by 6%. A nondegenerate, singly occupied level is induced in the bandgap at $E_C - 0.46$ eV (with a spin splitting of 0.07 eV).

Secondly, when the geometry optimization began with the N atom initially off the lattice site (in an arbitrary direction, without any symmetry constraints), the final structure had C_{3v} symmetry, in agreement with experiment and [11], which reported a similar calculation on a smaller cluster of 44 atoms. In the final structure, the N and unique C atoms relax away from each other along a ⟨111⟩ direction, the nitrogen–carbon bond elongating by 33% (28% in [11]). Two states are induced in the bandgap: one nondegenerate fully occupied level close to the valence band edge, at $E_V + 0.26$ eV ($E_V + 1.2$ eV in [11]), the other a singly occupied nondegenerate level at $E_C - 0.71$ eV ($E_C - 0.5$ eV in [11]). The spin splittings of these levels were 0.16 and 0.58 eV, respectively.

The relative energy difference between the on- and off-site nitrogen is 0.33 eV, the C_{3v} symmetry site having the lower energy and the T_d configuration being metastable.

Therefore, depending on the accuracy of the method and initial atomic positions used in the geometry optimization or dynamics calculation, either C_{3v} or T_d symmetry, or even both symmetries, may be found to be stable or metastable.

The effects of cluster size can be established by comparing these results with those of [11], where the same method has been used with a considerably smaller cluster: firstly the elongation of the unique N–C bond is seen to be larger in the larger cluster (most likely due to greater freedom for geometric relaxation of neighbours), while the partly occupied nondegenerate level is seen to drop lower in the bandgap. This is possibly partly due to the change in geometry (this level drops deeper in the bandgap with increasing distortion) as well as possible impurity–surface interactions. The fully occupied nondegenerate level above the valence band is found to be the most sensitive to cluster size, dropping from $E_V + 1.2$ eV in the 44-atom cluster of [11] to $E_V + 0.26$ eV in our 165-atom cluster calculations. This may be due to either the change in geometry or reduced impurity–surface interactions, or both.

2.3. Ab initio density functional theory, with periodic boundary conditions

The *ab initio* DFT calculations use the modern generalized gradient approximation (GGA) [38] with the state-of-the-art full potential linearized augmented plane wave (FLAPW) treatment as well as the augmented plane wave with local orbitals (APW + lo) [39] with fully relativistic treatment of core electrons, as implemented in the WIEN2k code [13]. Integration over the Brillouin zone used Blöchl's modified tetrahedron method [40]. In the (APW) group of methods the value of Rk_{max} (smallest muffin-tin radius multiplied by the maximum k-value in the expansion of plane waves) is an indication of the accuracy of the basis set used. Compared to the full potential linear augmented plane wave (FLAPW) method, smaller Rk_{max} can be used with the APW + lo approach, while maintaining the same accuracy [41].

For the pure diamond calculations a supercell of eight atoms was used with the FLAPW approach ($Rk_{max} = 8.0$), with 64 k-points in the full Brillouin zone to optimize the lattice parameter of pure diamond, which was found to be 3.49 Å (cf experimental value of 3.5667 Å [36]). The bandgap at the Γ-point was found to be 5.5 eV.

Calculations for the single substitutional nitrogen atom were performed for eight-atom and 64-atom periodic supercells, using the previously optimized lattice constant. The eight-atom calculation was performed using the FLAPW–GGA–DFT formalism. All atoms in the cluster were allowed to relax during geometry optimization, without any symmetry constraints.

Table 2. Summary of the ⟨111⟩ distortions of N and the axial carbon atom from their respective lattice sites in the eight-atom GGA–FLAPW and 64-atom GGA–APW–lo DFT calculations.

	8-atom cluster		64-atom cluster	
	Distortion from lattice site (Å)	Distortion as % of C–C bond length	Distortion from lattice site (Å)	Distortion as % of C–C bond length
Nitrogen	0.123	8.1	0.198	13.1
Unique carbon	0.197	13.1	0.227	15
Elongation of N–C bond	0.32	21.2	0.425	28.1

Table 3. Spin densities at atomic nuclei (within Thomson sphere) and within the atomic muffin-tin spheres in the 64-atom GGA–FLAPW–DFT calculation.

	Spin density at atomic nuclei	Spin density within atomic muffin-tin spheres
Nitrogen	0.281	0.151
Unique carbon	0.151	0.285
Neighbours of N	−0.001	−0.002
Neighbours of unique C	−0.015	−0.008

In the final geometry, the N and a unique C atom relaxed away from each other, yielding C_{3v} symmetry; these results are summarized in tables 1 and 2.

The 64-atom calculation was performed with the APW + lo GGA–DFT formalism. The cluster was constructed using $2\bar{2}\bar{2}$ conventional fcc diamond unit cells, with the previously optimized lattice constant, replacing one of the C atoms with a nitrogen atom. The symmetry of the cluster was restricted to C_{3v}, since the preliminary unconstrained eight-atom geometry optimization had found C_{3v} symmetry for the impurity, in agreement with experiment. 27 k-points were used in the full Brillouin zone, or six k-points in the irreducible wedge of the Brillouin zone, with $Rk_{max} = 5.0$. Increasing the number of k-points to 125 in the full Brillouin zone, no changes in the position of the impurity level in the bandgap or forces on the atoms were observed, while the spin density at the nuclei changed by less than 2.5%. Similarly, increasing the value of Rk_{max} did not result in changes in the optimized geometry.

Geometry optimization was performed, relaxing all atoms up to third neighbours of the nitrogen atom. The geometry optimization was continued until the forces on the atoms were smaller than 1 mRyd au^{-1} (0.026 eV $Å^{-1}$). Subsequently, the SCF cycles were continued until the total energy was converged to within 1×10^{-7} Ryd.

In the fully relaxed structure, the nitrogen atom relaxes away from its lattice site by 0.20 Å and the unique carbon by 0.23 Å along a ⟨111⟩ axis, towards the plane of their respective carbon neighbours. Hence the N–C bond elongates by 28%. The final geometry is shown in table 2.

Polarization of core electrons was found to have a significant contribution to the spin density at the atomic nuclei, this contribution reducing the valence electron contribution at N by 9.0 and 29.5% at the unique C atom, while increasing the valence electron contribution by 37.1% on the remaining C neighbours of N and 12.3% on the C neighbours of the unique carbon atom.

The spin densities on the atomic nuclei (within the Thomson sphere, since the core electrons are treated relativistically [42]), and the total spin densities within the muffin-tin

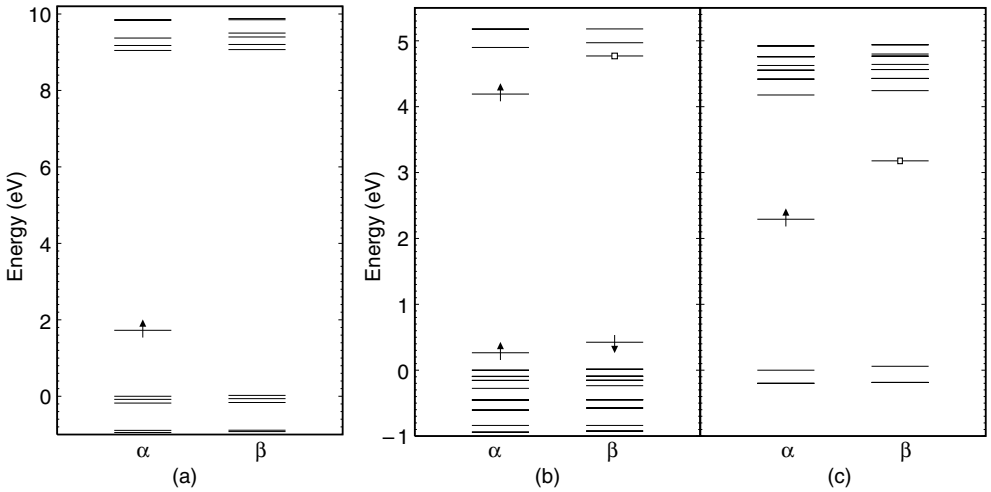

Figure 1. Energy levels of nitrogen impurity in diamond clusters of (a) 96 atoms (MNDO, periodic), (b) 122 atoms (LSDA–DFT, cluster) and (c) 64 atoms (APW + lo GGA–DFT, periodic). Energy levels are for the Γ-point of k-space and are relative to the Fermi level.

spheres, are given in table 3. The spin density at the nitrogen nucleus was found to be greater than the spin density at the unique C nucleus, in agreement with experiment [7]. On the other hand, the greater part of the spin density associated with the donor level wavefunction was found to reside in the vicinity of the unique carbon atom (∼65%), with ∼35% in the vicinity of the nitrogen atom (within the muffin-tin spheres of the respective nuclei), also in good agreement with experiment [8]. The spin densities in the vicinity of the nitrogen and unique carbon atoms is the reverse of the spin densities at the respective atomic nuclei. This is attributed to the fact that the nitrogen atom s orbital contributes more to the impurity wavefunction than the unique carbon atom s orbital (since only s orbitals have nonvanishing amplitude at atomic nuclei), while the reverse is true for the p orbitals.

The energy levels at the Γ-point of reciprocal space for the 64-atom cluster are shown in figure 1. We see that for spin up there is an impurity state, at 1.89 eV below the conduction band, slightly below the Fermi level (for spin down this level is at 1.07 eV below the conduction band, slightly above the Fermi level, due to spin splitting). This is the donor impurity state and its position is in good agreement with experiment [20], and with the calculations of Kajihara *et al* [10]. The density of states is given in figure 2 for the 64-atom periodic cluster including nitrogen, and also for pure diamond. The largest contributors to this energy level are the unique carbon's p orbitals, the nitrogen's p and s orbitals and the unique carbon s orbital (in that order). In addition, we find that the nitrogen generates a nondegenerate hyperdeep level at 1.5 eV below the bottom of the valence band, in agreement with other calculations [11, 32, 33].

The spin density associated with the impurity level is plotted in figure 3. It can be seen that the spin density is primarily associated with the impurity state. It is also seen that the donor level has an antibonding nature, with the electron density associated with this level having a node between the N and unique C atoms.

We can see some of the artifacts introduced by the small size of the cluster by comparing the eight- and 64-atom results. Both have a C_{3v} distortion, the N and unique C atoms shifting more in the 64-atom cluster, with the nitrogen–carbon distance correspondingly larger in the 64-atom cluster. The spin distributions are qualitatively similar, while the band structure is

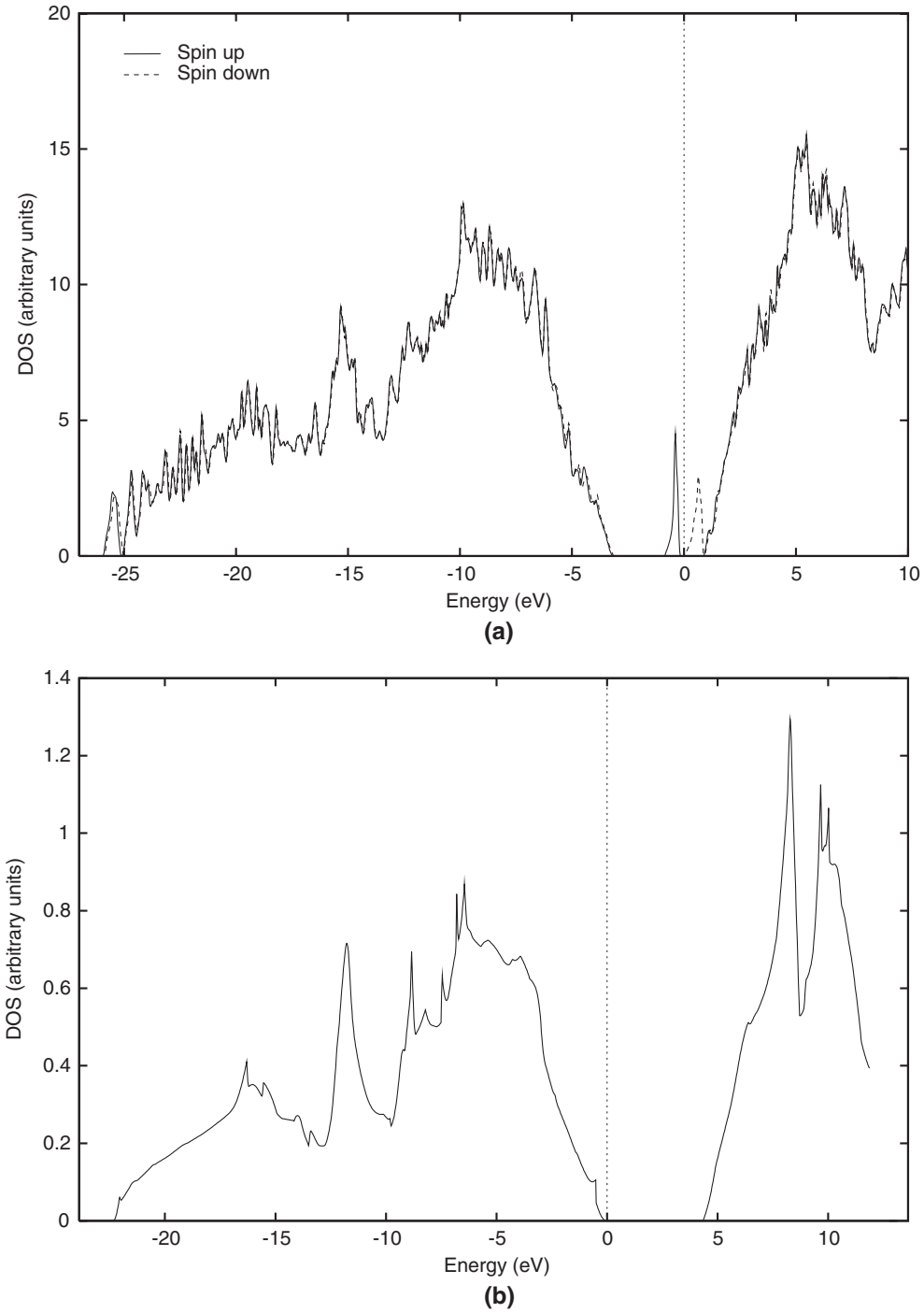

Figure 2. Density of states for the 64-atom GGA–DFT calculation (a) containing the single substitutional nitrogen and (b) for pure diamond. The full and broken curves show the up and down spin densities of states, respectively. Energies are relative to the Fermi level in each case, but, for clarity, plots (a) and (b) have been aligned such that the bandgaps coincide. In both cases 1000 k-points have been sampled in the full Brillouin zone using the modified tetrahedron method [40].

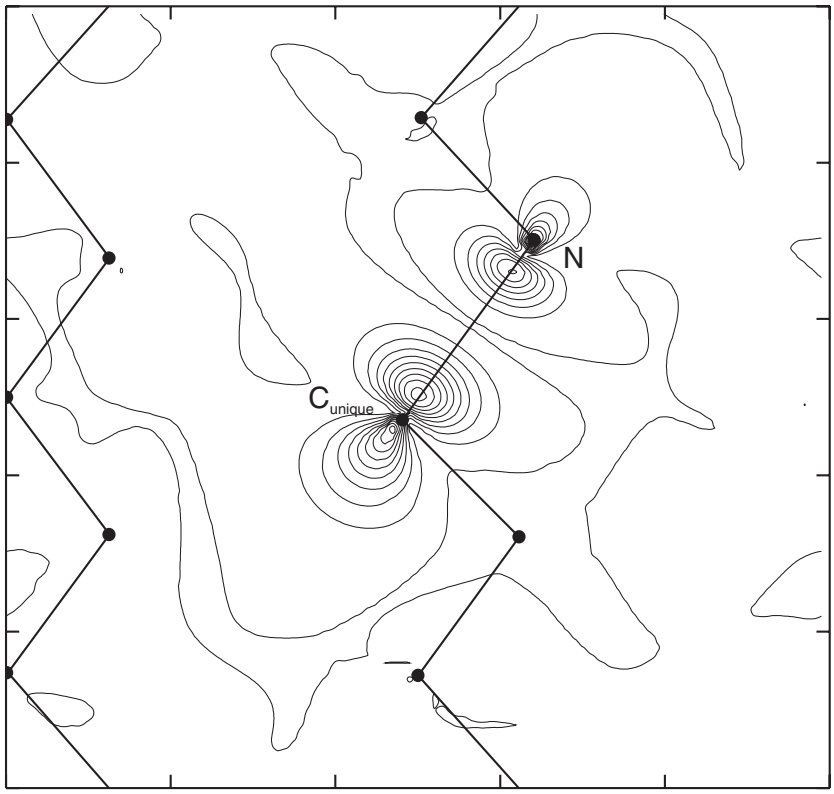

Figure 3. Spin density for the 64-atom periodic APW + lo GGA–DFT calculation. The plot passes through the nitrogen and unique carbon atoms in a (110) plane. The spacing between contours is 0.1 e $Å^{-3}$.

quite strongly dependent on cluster size. Hence, in agreement with other authors [10, 27, 33], it is seen that cluster size strongly influences the results, although qualitative agreement can be achieved for small clusters.

3. Discussion

The AM1 Hamiltonian based on the MNDO formalism reported here is the most advanced *semi-empirical* method that has been reported in the literature for calculations on single nitrogen in diamond. No distortion is predicted by this method, although other semi-empirical methods do predict the C_{3v} symmetry (though some on the basis of a Jahn–Teller distortion, which has since been shown to be incorrect).

On the other hand, more recent results from *ab initio* calculations have also been very mixed, with some calculations predicting no distortion, one calculation predicting no distortion of the nitrogen atom while its neighbours do distort and a majority of calculations predicting the C_{3v} distortion. There has been no *general* agreement as to the magnitude and origin of the distortion.

However, the new full potential all-electron 64-atom APW + lo model reported here is the first which agrees with a previous calculation (see [10], a pseudopotential plane wave model). In both cases an elongation of 28% has been obtained for the unique N–C bond, while the

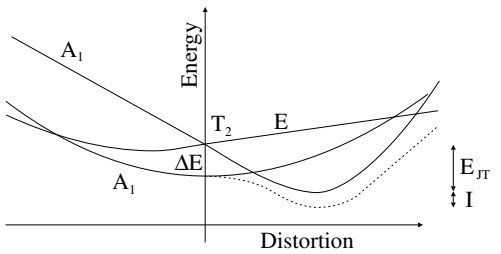

Figure 4. Schematic diagram of the expected energy level splitting when the T_d symmetry of a single nitrogen substitutional atom distorts into C_{3v} symmetry.

partially occupied one-electron level is found at $E_C - 1.9$ eV in both cases. These calculations do, however, differ with respect to the fully occupied nondegenerate level observed just above the valence band top in [10], but not observed in the bandgap in our calculations. This may be due to the pseudopotential methods used in the cases where this level has been observed in the bandgap (see [10] and also our finite cluster calculations of section 2.1), while a full core electron treatment was used in the APW + lo calculation where this level is not observed. In addition, our APW + lo calculations were performed using considerably more k-points. Considering this together with the sensitivity of this level to cluster size (section 2.1), it is seen that the position of this level is particularly sensitive to the approximations used.

Close examination of several of the models show that the discrepancies have one or more of the following causes.

(1) By symmetry, the nitrogen at the lattice site must be in equilibrium (although perhaps unstable). In order to demonstrate that it moves off site, the nitrogen must be displaced at the starting point of the calculation. Some calculations may not have done this or been able to do this [32, 33].
(2) The electronic orbitals of the nitrogen may hybridize into a filled 2s and three partially filled 2p orbitals. This will lead to the spin density located on the p orbitals on the nitrogen atom.
(3) Alternatively, the nitrogen's orbitals can form four sp^3 hybrids of which one is doubly occupied (the lone pair). The latter allows the three partially occupied sp^3 hybrids to bond with neighbouring carbon, leaving the lone pair and the unique carbon neighbour's dangling bond, which form completely occupied bonding and partially occupied antibonding orbitals. This is the conventional explanation of the P1 nitrogen EPR centre [10, 11, 43].

We can discriminate between cases 2 and 3 by looking at the p character of the unpaired electron.

It has been shown previously [26] that depending on the parametrization of specific semi-empirical methods, the position and order of energy levels in the bandgap may be altered. Considering this, it is seen that the properties of the P1 centre are delicately balanced. Hence if methods of differing accuracy are used to model the centre, different results could be obtained. Therefore the active electronic orbitals are very close in energy, and a crossover takes place to stabilize the distortion. Small changes in the parameters or the approximation scheme mean that this crossover of energy levels does not occur for the distortion concerned, and the defect relaxes back to the tetrahedral structure.

A qualitative picture (figure 4) of the problem is that the nitrogen's valence orbitals form sp^3 hybrids, which, in the crystal field, form an A_1 and a T_2 electronic state separated by ΔE.

There are also four sp^3 hybrids from the neighbouring carbons oriented towards the nitrogen. They form bonding and antibonding orbitals with the nitrogen sp^3 orbitals. The bonding orbitals are like normal carbon–carbon bonds and are therefore located in the valence band, or very low in the bandgap. There is one spare electron which must occupy an antibonding orbital—in a T_d environment this must be the symmetric A_1 electronic state. Under C_{3v} distortion the T_2 orbital splits into an A_1 and an E state, with the A_1 directed along the axis of the distortion. Since it is an antibonding orbital, the lengthening of the N–C bond lowers the energy of this A_1 state. Additionally, the configuration interaction between the two A_1 states will lower the compound state further, by energy I. As the N–C bond lengthens, the bonds to the other carbons move closer to a planar configuration, with more p character.

There are three quantities of importance: the crystal field splitting, ΔE, the Jahn–Teller-like reduction of energy of the A_1 state split from the T_2 state, E_{JT}, and the configuration interaction, I. Different computational systems and approximations will reproduce these in different ways. In particular, this explanation shows why some models which have no configuration interaction included may predict no distortion—a small C_{3v} distortion in figure 4 would relax back to the lattice site in the absence, or underestimation, of I.

It is also seen from [24] that nitrogen defects interact over long distances. This will have an influence on calculations using both periodic and nonperiodic clusters since the impurity–surface distance becomes important. Thus, it is important to use as large a cluster as possible, preferably one in which the repeat distance (for periodic clusters) or the defect–surface distance (for finite clusters) is greater than 7 Å (64-atom periodic cluster or ∼275-atom nonperiodic supercell).

4. Conclusion

Using the nitrogen impurity in diamond as an illustrative example, these calculations emphasize that care is necessary in searching for the global minimum structure of defects, such as by taking as starting points both symmetric and nonsymmetric structures, to ensure that the defect can relax into a global, not a local, minimum. This is most important for cases where the geometry of the centre is not known in advance since an initial geometry that leads to a local minimum could easily be selected.

Cluster size is important, but even more so are the approximations in the method (calculations on small clusters using *ab initio* methods gave better results than those on larger clusters using more approximate methods). In addition, the size of the cluster, periodic or finite, must be sufficient to minimize defect–defect or defect–surface interactions. We note that the models based on DFT reported in this work give a good model of nitrogen in diamond, with the model based on the highest level of theory yielding the best results. We also observe that the researchers with most experience of the material tend to obtain the best results.

The full potential APW + lo calculations reported here and the pseudopotential calculations of [10] are the first where agreement is found for the elongation of the unique N–C bond (28%) and position of the partially occupied one-electron level in the bandgap ($E_C - 1.9$ eV), though this agreement does not extend to the partially occupied nondegenerate level above the valence band.

From the full potential, all-electron APW + lo calculations reported here, polarization of core electrons was found to have a significant contribution to the spin density at the atomic nuclei. This contribution reduced the valence electron contribution at N and the unique C atoms by 9.0 and 29.5%, respectively, while increasing the valence electron contribution on the remaining C neighbours of N and of the unique C atom.

The spin density at the N nucleus was found to be greater than the spin density at the unique C nucleus, in agreement with experiment, while the greater part of the spin density

associated with the donor level wavefunction was found to reside in the vicinity of the unique carbon atom (within the muffin-tin spheres of the respective nuclei), also in good agreement with experiment. The spin densities in the vicinity of the nitrogen and unique carbon atoms is the reverse of the spin densities at the respective atomic nuclei, which is attributed to the fact that the nitrogen atom s orbital contributes more to the impurity wavefunction than the unique carbon atom s orbital (since only s orbitals have nonvanishing amplitude at atomic nuclei), while the reverse is true for the p orbitals.

In conclusion, it is clear that computational calculations, however sophisticated the method, are fallible, although at their best they can give a very useful, complete model of a defect.

Acknowledgments

We thank W S Verwoerd for his many useful suggestions and constructive criticism. AM would like to thank staff at UNISA for their hospitality during her stay there. We also thank R Jones and P R Briddon for permission to use the AIMPRO code.

References

[1] Kohn W and Sham L J 1965 *Phys. Rev.* A 1133
[2] Dewar M J S, Zoebisch E G, Healy E F and Stewart J J P 1985 *J. Am. Chem. Soc.* **107** 3902
[3] Sellschop J P F 1992 *The Properties of Natural and Synthetic Diamond* ed J E Field (London: Academic) p 81
[4] Kiflawi I and Bruley J 2000 *Diamond Relat. Mater.* **9** 87
[5] See, for example
Johnston K, Mainwood A, Collins A T, Davies G, Twitchen D J, Baker J M and Newton M E 1999 *Physica* B **273/274** 647
Kang D 1998 *Bull. Korean Chem. Soc.* **19** 628
[6] Collins A T 1999 *Diamond Relat. Mater.* **8** 1455
[7] Smith W V, Sorokin P P, Gelles I L and Lasher G J 1959 *Phys. Rev.* **115** 1546
[8] Farrer R G 1969 *Solid State Commun.* **7** 685
[9] Messmer R P and Watkins G D 1973 *Phys. Rev.* B **7** 2568
[10] Kajihara S A, Antonelli A, Bernholc J and Car R 1991 *Phys. Rev. Lett.* **66** 2010
[11] Briddon P R, Heggie M I and Jones R 1992 *Mater. Sci. Forum* **83–87** 457
[12] Stewart J J P 1993 *MOPAC 93.00 Manual* (Tokyo: Fujitsu)
[13] Blaha P, Schwarz K and Luitz J 1999 *WIEN97, A Full Potential Linearized Augmented Plane Wave Package for Calculating Crystal Properties* Technical University of Vienna (ISBN 3-9501031-0-4)
This is an improved and updated Unix version of the original copyrighted WIEN code, which was published by
Blaha P, Schwarz K, Madsen G K H, Kvasnicka D and Luitz J 2001 *WIEN2k, an Augmented Plane Wave + Local Orbitals Program for Calculating Crystal Properties* ed K Schwarz Technical Universität Wien, Austria (ISBN 3-9501031-1-2)
[14] Jones R and Briddon P R 1998 *Identification of Defects in Semiconductors: Semiconductors and Semimetals* vol 51A, ed M Stavola (New York: Academic) ch 6 p 287
[15] Loubser J H N and van Wyk J A 1978 *Rep. Prog. Phys.* **41** 1201
[16] Barklie R C and Guven J 1981 *J. Phys. C: Solid State Phys.* **41** 3621
[17] Cox A, Newton M E and Baker J M 1994 *J. Phys.: Condens. Matter* **6** 551
[18] Loubser J H N and Du Preez L 1965 *Br. J. Appl. Phys.* **16** 457
[19] van Enckevort W J P and Versteegen E H 1992 *J. Phys.: Condens. Matter* **4** 2361
[20] Ammerlaan C A J 1981 *Inst. Phys. Conf. Ser.* **59** 81
[21] Loubser J H N and Van Ryneveld W P 1967 *Br. J. Appl. Phys.* **18** 1029
[22] Reynhardt E C, High G L and van Wyk J A 1998 *J. Chem. Phys.* **109** 8471
[23] Zaritskii I M, Bratus V Ya, Vikhnim V S, Vishnevskii A S, Konchits A A and Ustintsev V M 1976 *Sov. Phys.–Solid State* **18** 1883
[24] Nadolinny V A, Yelisseyev A P, Baker J M, Twitchen D J, Newton M E, Hofstaetter A and Feigelson B 1999 *Phys. Rev.* B **60** 5392

Nadolinny V A, Yelisseyev A P, Badalyan A G, Baker J M, Twitchen D J, Newton M E, Hofstaetter A and Feigelson B 1999 *Diamond Relat. Mater.* **8** 1565
[25] Astier M, Pottier N and Bourgoin J C 1979 *Phys. Rev.* B **19** 5265
[26] Lannoo M 1982 *Phys. Rev.* B **25** 2987
[27] Mainwood A 1978 *J. Phys. C: Solid State Phys.* **11** 2703
[28] Mainwood A 1979 *J. Phys. C: Solid State Phys.* **12** 2543
[29] Mainwood A 1994 *Phys. Rev.* B **49** 7934
[30] Sahoo N, Mishra K C, van Rossum M and Das T P 1987 *Hyperfine Interact.* **35** 701
[31] Jackson K, Pederson M R and Harrison J G 1990 *Impurities, Defects and Diffusion in Semiconductors: Bulk and Layered Structures (MRS Symp. Proc. No 163)* ed D J Wolford, J Bernholc and E E Haller (Pittsburgh, PA: Materials Research Society) p 89
[32] Bachelet G B, Baraff G A and Schlüter M 1981 *Phys. Rev.* B **24** 4736
[33] Erwin S C and Pickett W E 1990 *Phys. Rev.* B **42** 11056
[34] Nishimatsu T, Katayama-Yoshida H and Orita N 1996 *23rd Int. Conf. on Phys. Semicond.* vol 4, ed M Scheffler and R Zimmermann (Singapore: World Scientific) p 2581
[35] Miyamoto Y and Saito M 1998 *Phys. Rev.* B **57** 6527
[36] Donnay J D H and Ondik H M 1973 *Crystal Data: Determinative Tables* vol 2, 3rd edn US Department of Commerce–National Bureau of Standards–JCPDS
[37] Bachelet G B, Hamann D R and Schlüter M 1982 *Phys. Rev.* B **26** 4199
[38] Perdew J P, Burke S and Ernzerhof M 1996 *Phys. Rev. Lett.* **77** 3865
[39] Sjöstedt E, Nordström L and Singh D J 2000 *Solid State Commun.* **114** 15
[40] Blöchl P E, Jepsen O and Anderson O K 1994 *Phys. Rev.* B **49** 16223
[41] Madsen G K H, Blaha P, Schwarz K, Sjöstedt E and Nordström L 2001 *Phys. Rev.* B **64** 195134
[42] Blügel S, Akai H, Zeller R and Dederichs P H 1987 *Phys. Rev.* B **35** 3271
[43] Stoneham A M 1992 *The Properties of Natural and Synthetic Diamond* ed J E Field (London: Academic) p 3